DOI: 10.61782/fa.2025.0170

BENCHMARKING ROOM ACOUSTIC SOUND PARTICLE SIMULATIONS INCORPORATING UNCERTAINTY-BASED DIFFRACTION: CHALLENGES AND STRATEGIES

Iván Herrero-Durá[1*] **Thomas Judd**[1] **Stefan Weigand**[1]
Jasmin Hörmeyer[1] **Jochen Schaal**[1]
[1] SoundPLAN GmbH, Etzwiesenberg 15, 71522 Backnang (Germany)

ABSTRACT

Outdoor noise prediction methods are standardized and well-defined due to their regulatory applications, ensuring reliable and comparable results. Benchmark test cases for validating software implementations are therefore straightforward to define and widely accepted as a quality management tool. In contrast, room acoustics presents different challenges. The diversity of algorithms and methods for predicting sound propagation and key metrics such as reverberation time (RT) or speech transmission index (STI) increases the complexity of benchmarking. Competing approaches strive to incorporate complex physical phenomena while keeping computational aspects within feasible limits, making method-agnostic comparisons of results essential. The need for reference solutions that systematically evaluate all aspects of sound propagation while remaining generally valid significantly narrows the scope of potential benchmarks. Four primary approaches are discussed for obtaining reference values: analytical solutions, numerical simulations, experimental measurements, and round-robin comparisons. In this paper, test cases are presented by employing these approaches, which have successfully been used to validate geometrical room acoustic models. These examples highlight the importance of strategic benchmark design in advancing the reliability and comparability of room acoustic simulation tools. The challenges posed by room acoustics are highlighted, including complex diffraction phenomena, and potential approaches are proposed to address these challenges.

*Corresponding author: *ivan.herrerodura@soundplan.de.*

Keywords: *sound particle method. uncertainty-based diffraction, room acoustic simulation.*

1. INTRODUCTION

Quality control for outdoor noise prediction methods is generally achieved through algorithmic prescription, described in official guidelines. Partly for historical reasons, and partly due to additional flexibility in terms of mathematical modelling options, this is not a feasible course to take with indoor noise and room acoustic prediction methods. In the absence of a fixed algorithm, target results are required for benchmarking. This presents additional challenges since analytical and numerical approaches may omit certain physics and when comparing with measurements, systematic differences and uncertainties complicate matters, especially at low frequencies.

Traditionally, simulation of indoor sound propagation and room acoustic metrics have been done with geometric acoustic methods where sound rays are modelled as straight lines and phase is neglected. Diffraction is implicitly lacking. It can be reinserted using additional (usually empirical) algorithms but many current methods are only comfortable with up to a couple of diffraction events. This approach allows reasonable estimates with acceptable computational effort for a wide range of scenarios, but at the cost of neglecting wave physics.

By contrast, wave-based methods such as FDTD or FEM/BEM, among others, include interference effects and diffraction implicitly but have proved cumbersome to employ in larger situations and have issues with boundary definition.

As an interesting alternative that occupies a middle ground between these two ends of the spectrum, sound particle methods with uncertainty-based diffraction (Sound Particle Diffraction, SPD) [1] offer similar computational requirements to the geometrical methods. However, like wave-based methods, the rules of the simulation can remain the same at all times and places with diffraction always on, to arbitrary order. This methodology has been operational for many years in the indoor module of the commercial software for noise control SoundPLAN-noise. Detailed information about its implementation and testing can be found in references [2–5].

The Sound Particle Diffraction method has a particular usefulness in the context of establishing validation references, since diffraction can be set to always-on, always-off, or any number of diffraction orders in between. It can therefore assess the importance of diffraction in a reference case and hence offer insight into the extent to which a test case can be used for both wave-based and geometric methods.

In this paper, test cases are presented, which contribute to the four categories available to method-agnostic testing. In the area of analytic testing, we show how BTM-based theory (as implemented in the Svensson group's ESIE edge diffraction toolbox) relates to the Maekawa approach. In the area of simulations we demonstrate that sound particle methods can offer good agreement with analytical references in non-trivial geometries, but certain conditions must be fulfilled to ensure comparison of like with like. These conditions have strong relevance for round-robin comparisons since we present cases where agreement is not possible between methods where diffraction is always on and those that can only handle a small number of (or no) diffraction events. Finally we turn to measurements and show cases where these can offer useful benchmarks for non-trivial cases, but we also discuss limitations.

As a final point, it is shown that Speech Transmission Index results can be less sensitive to the physics employed in a method. However, limitations of this metric for validating simulations are also discussed.

2. SPD ALGORITHM REVISITED

The sound particle method used in this paper corresponds to that developed by Stephenson [6], later extended in the work of Judd *et al*. [3]. The reader is referred to the reference for details. To summarize: the method is from the ray-tracing family and implements geometrical acoustics including specular and diffuse reflections (governed by a Monte Carlo Lambert scheme), Poissonian room scattering, statistical transmission through walls, and uncertainty-based diffraction. Diffraction is implemented by first obtaining the bypass distance as a sound particle flies by a diffracting edge with incidence angle ε. This is then used to calculate an effective slit width b (a function of the currently considered wavelength), which is then plugged into a weighted probability distribution function with normalization constant D_0 to determine the new particle direction. Although alternatives are available, much use has been made of the function

$$D(\nu) = \frac{D_0}{(1 + 2\nu^2)}, \tag{1}$$

where $\nu = 2b\varepsilon$. This formula has connections with Fraunhofer diffraction but is best regarded as empirical. Various options regarding how to limit the outgoing angle have been explored - we prefer to allow a full angle range ($-\pi$ to π) to avoid discontinuities in the sound field and approximate limited transmission through apertures smaller than the wavelength under consideration. A useful feature of the formula is that it can be empirically calibrated to benchmarks by weighting b appropriately.

3. CASE STUDIES

Seven test cases that compare sound particle simulation results with reference values are presented, the first five relating to cases in the DIN 38457, and the last two based on measurements previously performed in a semi-anechoic chamber [7]. For the sake of conciseness, the reader is referred to the DIN 38457 standard for more details on the models presented below. The DIN cases have an analytical basis but the tolerance zones were typically determined through round-robin simulations, hence these examples cover a broad range of reference categories.

3.1 Benchmark 1: Determination of the absorption of a baffle arrangement in a reverberation chamber

The test case presented below allows the SPD model to be validated for random incidence in a diffuse field. This case corresponds to T07 of DIN 38457 and considers an arrangement of baffles in a reverberant room, the aim being to determine the overall sound absorption of the baffle system.

The baffles are placed in 6 rows of 3.6 m length, rotated in the test setup by 30° in relation to the vertical axis at its center. The baffles are arranged with a vertical extension of 0.45 m at a row center distance of 0.45 m as well. The arrangement is enclosed by a frame with a scattering coefficient of 0.0 (specular reflection) and an absorption coefficient of 0.0. The absorption coefficient of the room walls is 0.05 with a 1.0 scattering coefficient.

In this scenario different factors come into play that can be taken into account when determining the absorption of the baffles in a reverberant room. These are the reflective floor of the room, diffraction and sound absorption by the air. Here, four different combinations of these factors are explored, keeping the reflective floor of the room as the only constant parameter of these three (Table 1).

Table 1. Combination of factors for the determination of the absorption of a baffle arrangement in a reverberation chamber. RF: reflective floor, Diff: diffraction, α_{air}: air absorption.

Case	RF	Diff	$\alpha_{\mathbf{air}}$
1	X		
2	X	X	
3	X		X
4	X	X	X

From the theory presented in the DIN 38457, the expected analytical result for this test case is $\alpha_p = 0.83 \pm 0.1$, the tolerance region having been determined from round-robin investigations. Figure 1 shows the results obtained using the SPM model, as well as the limits indicated by the standard for the validity of the model. One can observe here that there are two cases that fall between the defined intervals in the full frequency range, while two others only do so from 2000 Hz onward. The two cases that meet the standard are those in which diffraction has not been considered as a parameter in the calculation, regardless of the consideration of sound absorption by air. If diffraction is neglected, as in the theory, the agreement between the analytical value of 0.84 and simulation is on the order of 1%, a gratifying result considering that the geometry is non-trivial.

When always-on diffraction is incorporated, the low frequencies deviations from the analytical result are unsurprising because the wavelengths are similar in size to (or larger than) the spacing between the baffles. As has been shown by Bethe [9] and others, the energy of the incident wave will not fully transmit through the slit under these conditions, and therefore not fully enter the strongly absorbing zone.

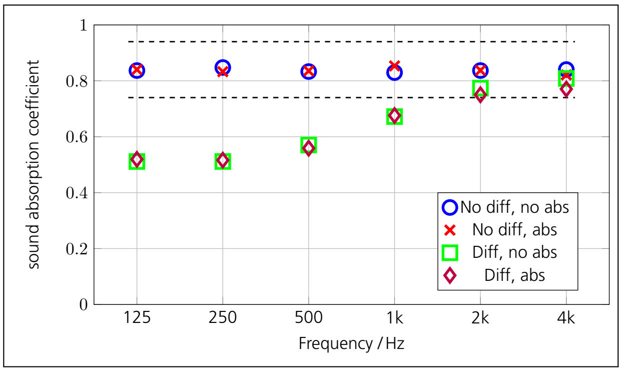

Figure 1. Sound absorption coefficient calculated with different combinations of factors: no diffraction, no air absorption (blue circles), no diffraction, air absorption (red crosses), diffraction, no air absorption (green squares) and diffraction, air absorption (magenta diamonds). The black dashed lines indicate the lower and upper bounds specified by the DIN 38457.

Restricting SPD to one diffraction event still gives reasonable agreement. Unlike the coupled room case (introduced in Section 3.2), air absorption does not strongly influence the results because the results are compared at the same physical location.

3.2 Benchmark 2: Sound transmission between coupled rooms

The sound transmission between rooms that are connected by an aperture is studied in the following case, corresponding to the T08 in the DIN 38457. The test arrangement consists of two adjacent reverberant chambers, each measuring 6 m × 6 m × 6 m, separated by a central partition with a 2 m × 2 m opening. The absorption coefficient of all boundary surfaces is 0.05, while the scattering coefficient is set to 1.

According to the standard, the theoretical value of the sound level difference between the two rooms under the indicated conditions is 5.6 dB. Following round-robin numerical simulations, a tolerance zone of ± 0.3 dB for a frequency-averaged result was established. Figure 2 shows the obtained level difference in the described situation.

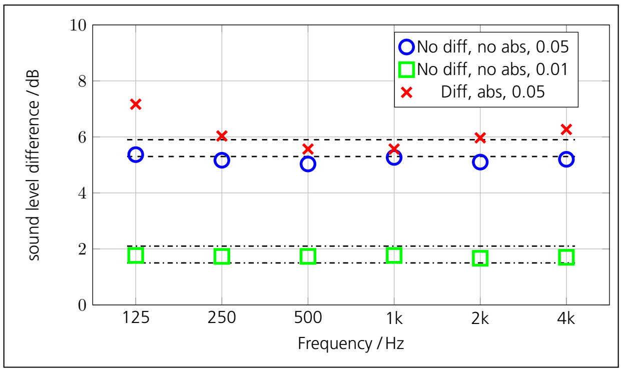

Figure 2. Sound level difference between two coupled rooms obtained without (blue circles) and with (red crosses) diffraction for a sound absorption coefficient in the boundary surfaces of 0.05, and without diffraction (green squares) for a sound absorption coefficient in the boundary surfaces of 0.01. Black dashed and dashed-dotted line show the tolerance values of both cases.

One can note that with diffraction and air absorption turned off (blue circles), the simulation results are slightly outside the tolerance zone. This is because in this test case, the absorption coefficient of the walls is 0.05, and this is enough to cause deviations from the perfectly diffuse sound field upon which the theory governing the test case is based. To prove this, results for the test case with a 0.01 absorption coefficient are shown, revealing closer agreement between the simulation and analytical theory. The curve with red crosses shows the simulation results with always-on diffraction and air absorption. We see that the level difference is a little higher for both lower and higher frequencies under these conditions. The lower frequency deviations are due to the limitation of transmission when the wavelength is no longer much smaller than the aperture, as discussed in the baffle test case. The higher frequency discrepancies are due to the fact that we compare between receivers in different locations and the average path length at the point when a particle strikes a receiver is higher in the second room than in the first room with the source, hence the stronger air absorption at high frequencies is significant.

3.3 Benchmark 3: Sound propagation with shielding in free field

In this case, the insertion loss, IL, for a single diffraction event is calculated by using the SPD method, the Biot-Tolstoy-Medwin (BTM) diffraction model [10] (as implemented by the Svensson group in their Edge Diffraction Toolbox) and Maekawa's model [11]. Specifically, the BTM diffraction model illustrates the Lagrangian technique of using normal coordinates in the context of infinite spaces subject to the laws of mechanics. The main potential of this method lies in its generality, being applicable even in non-separable coordinate systems. On the other hand, Maekawa described a method based on an approximate theory of optical diffraction for calculating the shielding effect of a real screen employed for the purpose of noise reduction. This method deals not only with diffraction phenomena, but also with reflections from the ground.

The geometry of the test case is similar to the test case T09 in the norm DIN 38457, "sound propagation with shielding in free field", but with a higher ceiling to better match the assumptions of BTM theory. The model consists of a fully absorbing room (all the walls having a sound absorption coefficient of $\alpha = 1$), a sound source, S, five receivers, R_1 to R_5, and a screen, B. The sound source emits pink noise with the sound power level indicated in the above cited DIN standard. The receivers are located at a height of 0.8 m above the ground and at a distance from the screen of 0.55 m, 1,55 m, 2.55 m, 3.55 m and 4.55 m, respectively.

The calculation of the sound pressure levels at the five locations for the octave frequency bands from 125 Hz to 4000 Hz is carried out both without a screen (giving in each case the free-field level, L_1) and with a screen (sound pressure level with diffraction, L_2). The IL is calculated from these two parameters.

The results are shown in Figure 3. In this case we use the analytical results as a reference to tune the function that sets the effective slit width. To improve the visualization of the results, only the two extreme cases are shown, i.e. those located closest to and farthest from the screen (receivers 1 and 5). The results show that such a calibration can work well across a range of frequencies and positions.

In this particular case, with fairly modest diffraction angles, the Maekawa reference is similar to the more sophisticated BTM theory with deviations on the order of a couple of decibels. The SPD results reveal that calibration

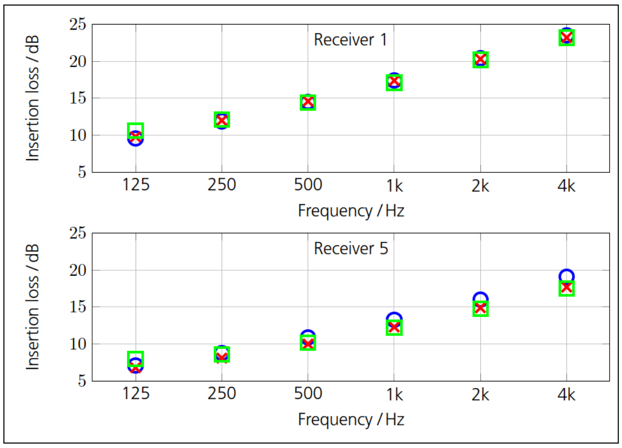

Figure 3. Insertion loss obtained with the BTM (blue circles), Maekawa (red crosses) and SPD (green squares) models.

using the effective slit width allows the method to track these reference results. The slight deviations are within acceptable bounds and are not relevant in the context of general uncertainties in the field.

3.4 Benchmark 4: Sound propagation in rooms densely occupied by objects

The model proposed in this case corresponds to the T10 in the DIN 38457. The purpose of this case is to study the suitability of a method to properly determine sound propagation in a space with a high density of obstacles, such as industrial halls with machinery and technical facilities. It consists of a room with dimensions 30 m x 30 m x 6 m (L x W x H) in which 63 cuboids, each measuring 1.5 m x 1.5 m x 5 m, are arranged upright on the floor and parallel to the axes in the room. The line of blocks between two of the corners of the room are removed so that a free diagonal path remains. The objects have a minimum distance of 1.5 m from the source to the receiver path. The surfaces of the cuboids standing on the floor are assigned a scattering coefficient of 1.0 and an absorption coefficient, α_s, given in the VDI 3760 standard [13].

There is a related test case in the VDI 3760 and an analytical benchmark is available that uses a single, overall coefficient for the scattering object density. As such, the DIN 38457 test case, with its specifically defined objects, represents an approximation to this. When waves impinge on an object, longer wavelengths result in a larger scattering cross-section owing to diffraction effects so we may expect differences between low-frequency and high-frequency results. Such effects could in theory be incorporated in the analytic theory through appropriate adjustment of the scattering object density, which implicitly includes the scattering cross-section, so it is worth quantifying these differences. If threshold frequencies might be found above which diffraction is shown to play little role, such test cases could be used to test a broader range of methods.

Figure 4 shows the sound level difference obtained by deducting the cases with and without diffraction. One can observe here that diffraction does not play a relevant role in the sound propagation at higher frequencies, such as 4000 Hz, presenting a difference of ± 0.7 dB between the with and without diffraction cases. This situation changes when analyzing the lower frequencies. In these cases, the sizes of the cuboids and the distance between them are of the same order of the wavelength, producing greater scattering and, consequently, variations between the diffracting and non-diffracting cases of up to ± 5 dB.

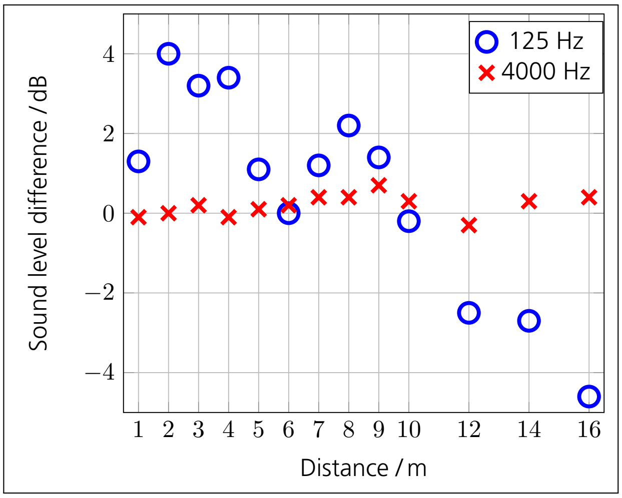

Figure 4. Sound level difference obtained by deducting the cases with and without diffraction for 125 Hz (blue circles) and 4000 Hz (red crosses).

The effect of increased scattering cross-section due to diffraction acts to restrict the propagation of sound along the first half of the sound propagation curve, resulting in higher level values nearer the source. This is subsequently compensated by less sound energy arriving at points further away from the source. There are fluctuations in the results due to the fact that at various points along the propagation curve, cuboids come closer to the path than at other points. The curve was truncated at 16 m to avoid possible corner effects.

In Figure 5 we plot the simulation results along with the reference theory for 125 Hz and 4000 Hz. This confirms once again that in spite of the complicated geometry and approximations with respect to the analytical theory, this test case is an effective test of geometric sound propagation methods.

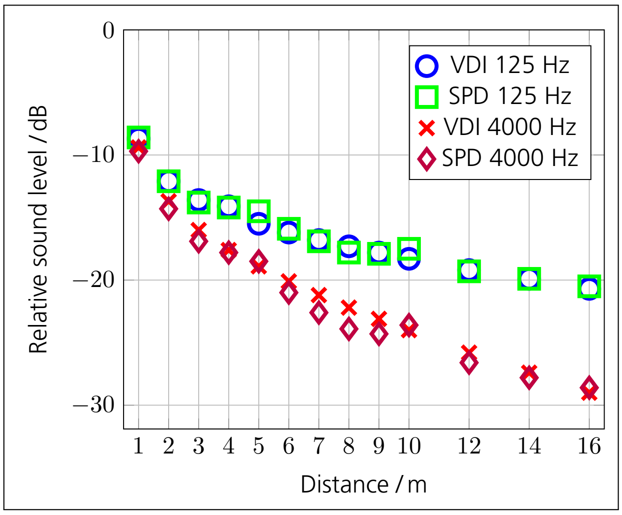

Figure 5. Relative sound level in the TA10 test case for the VDI at 125 Hz (blue circles), the VDI at 4000 Hz (red crosses), the SPD at 125 Hz (green squares) and SPD at 4000 Hz (magenta diamonds).

3.5 Benchmark 5: Calculation of the speech transmission index with room influence for diffuse field conditions

The speech transmission index, STI, evaluates the intelligibility of speech for a person located in a given position in a room by a listener located in a different position. The result of the evaluation is a number between 0.0 and 1.0, where the former means absolute unintelligibility and the latter means the best possible intelligibility [12].

Test task T12 of the standard offers three possible cases (T05, T06 and T07) with which to test the methodology used, all of them in a reverberation chamber inspired by test tasks described in the document itself. In this case, the SPD method has been applied to task T07, introduced in Section 3.1 of this work, and the STI has been calculated both disregarding and considering diffraction. In contrast with the reverberation time results, the STI results for the baffle system are only slightly affected by diffraction, the results being 0.49 without diffraction and 0.47 with diffraction. Diffraction decreases absorption by the baffles due to less-than-100% transmission into the absorbing zone. Nonetheless, this has less effect on STI than other results because only low frequencies deviate strongly and STI incorporates higher frequencies (which carry more weight) to produce a combined result.

3.6 Benchmark 6: Comparison with a single screen in semi anechoic chamber

At some point, finding suitable references becomes difficult, particularly as the geometry of the case grows more complex or when increasingly intricate acoustic phenomena – such as diffraction combined with reflection, or multi-path, multi-order diffraction – must be considered. In such cases, measurements can serve as valid references, even though they come with their own challenges and limitations, including discrepancies between the real-world scenario and its modelled representation. These challenges may be practical in nature, such as inaccuracies in determining source or receiver positions, limited knowledge of the actual absorption properties of materials used, measurement uncertainties, or differences caused by propagation phenomena not accounted for in the numerical model.

Here, we present results from a case that involves diffraction around a quasi-infinite reflective screen, combined with floor reflections [7]. The screen height is 1.5 m; the source and receivers are positioned in a plane orthogonal to the screen, centered along its midpoint. The source is placed at a height of 1.0 m and located 1.5 m in front of the screen. Thirty-one receivers are arranged in four columns, labeled A through D, with column A being the furthest from the screen and column D directly in front of it. Figure 6 shows the insertion loss results over the receiver height relative to the screen height for the 1 kHz octave band. The results demonstrate that SPD is capable of accurately reproducing the measurements. While some deviations are observable near the floor – where the simulation overestimates the received energy – this confirms that the method effectively handles diffraction in combination with reflections.

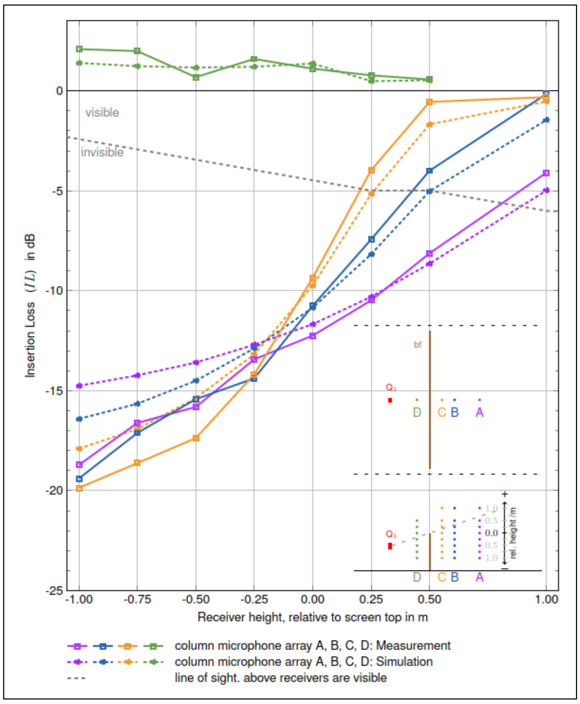

Figure 6. Comparison of measured and simulated insertion loss for the 1 kHz octave band around a quasi-infinite reflective screen in a semi-anechoic chamber, including ground reflection for 31 receivers, arranged in four columns A to D.

3.7 Benchmark 7: Comparison to two screens in zigzag configuration in semi an-echoic chamber

Finally, we turn to a scenario for which no reference exists other than measurement, as it cannot be modelled using any of the reference calculation methods. We examine sound propagation in a two-screen zigzag configuration, where two reflective screens are arranged with an overlap, creating a weaving pathway between them. Similar setups are often encountered in real-life situations, such as pedestrian walkways that cross noise barriers along roads. This configuration involves multiple propagation paths and higher-order diffraction, with sound traveling both over the two barriers and through the weaving path, which forces rays to bend twice in opposite directions. Additionally, multiple reflections between the two screens and the reflective floor may occur. Maekawa's method is not designed for such a complex geometry.

The same four receiver columns are used in this scenario. Columns C and D are positioned between the two screens, while the remaining two are placed behind the second screen. As before, the source and receivers are located in the central plane orthogonal to the screen arrangement. Figure 7 shows the insertion loss results for the 1 kHz octave band.

The results indicate that the SPD method reproduces most of the measurement results to within a tolerance of $\sim$ 2 dB but some positions show greater discrepancies. Notably, the receivers located between the two screens still follow the general trend, despite greater deviation compared to the single-screen case. This demonstrates that the SPD method can qualitatively reproduce even such a complex scenario.

Some of the observed deviations at individual receiver positions could be attributed to interference effects occurring near the floor or the reflective screens, as noted in other experiments. Since interference is not represented in an energetic physical model, the simulation cannot replicate these effects.

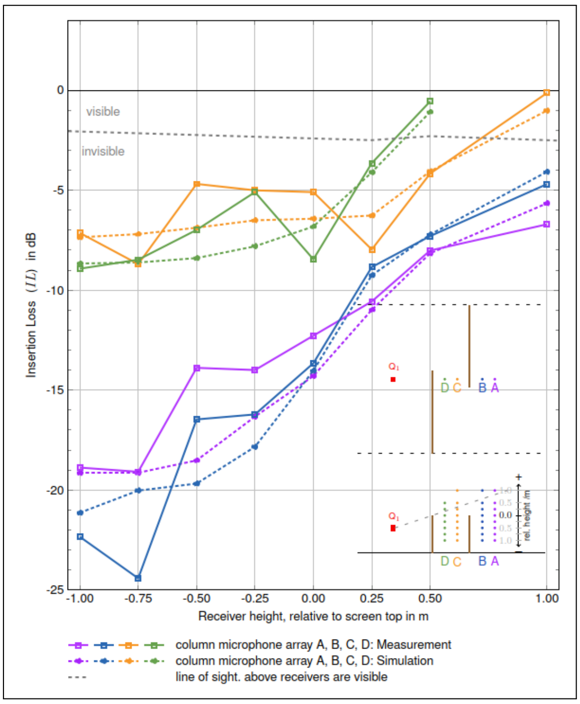

Figure 7. Comparison of measured and simulated insertion loss for the 1 kHz octave band in a zigzag two-screen configuration within a semi-anechoic chamber, including ground reflection.

4. CONCLUSIONS

We have shown that in a number of test cases with non-trivial geometry, useful analytical benchmarks for geometrical acoustic approaches exist and that sound particle methods can be in good agreement with these. This agreement is conditional on comparing like with like so in cases where the analytical reference is calculated in absence of effects such as diffraction and air absorption, the simulation must impose similar rules. In cases where a perfectly diffuse sound field is assumed in a theory, an overall absorption coefficient of 0.05 is already enough to produce noticeable deviations from expected results.

Hence, we revealed that while it is of great value to have analytical references, their usefulness at low frequencies may be limited to geometrical methods since wave-based methods generally include diffraction implicitly, and as such, it cannot be turned off. This suggests that wave-based methods will require greater use of measurements and wave-based analytical theories to test them. For round-robins with geometric methods, the simulation settings must be carefully agreed in advance, taking the role of diffraction into account. STI results are less sensitive to such issues, but they are a less stringent probe of low frequency effects and are less sensitive, generally.

In spite of these difficulties, we have noted that results at 4000 Hz were little affected by diffraction. This may help in devising test results that a broad range of simulation methods can agree with.

We have shown that in spite of known problems with the Maekawa empirical formula, it agrees fairly well with BTM-based methods in the DIN test case T09. We also demonstrated that the sound particle method could be calibrated to track both references.

Finally we show that measurements can offer benchmarks with which geometric methods can reasonably agree, but there are also cases where discrepancies are larger, presumably due to uncertainties and wave-based physical effects.

5. REFERENCES

[1] U. M. Stephenson. Simulation of multiple Sound Particle Diffraction based on the Uncertainty Relation - a revolution in noise immission prognosis; Part I: Principle and Method. In *Proc. of Euronoise 2018* , pages 2063–2076, Crete, Greece, 2018.

[2] T. Judd and J. Schaal. Recent advances in sound particle methods. In *Proc. of Internoise 2020* , Seoul, South Korea, 2020.

[3] T. Judd, D. Zollitsch, S. Weigand, U. Stephenson and J. Schaal. Uncertainty-based diffraction using sound particle methods in noise control software. In *Proc. of Internoise 2016* , pages 1050–1058, Hamburg, Germany, 2016.

[4] J. Schaal and T. Judd. Dealing with anomalous diffraction behaviour in noise standards using sound particle diffraction. In *Proc. of DAGA 2017* , pages 264–266, Kiel, Germany, 2017.

[5] J. Schaal and T. Judd. A 3D sound particle model with uncertainty-based diffraction for general geometries. In *Proc. of ICSV24* , London, UK, 2024.

[6] U. M. Stephenson and U. P. Svensson. An improved energetic approach to diffraction based on the uncertainty principle. In *Proc. of the 19th International Congress on Acoustics* , Madrid, Spain, 2007.

[7] S. Weigand, U.M. Stephenson, J. Schaal. Simulation of multiple Sound Particle Diffraction based on the Uncertainty Relation - a revolution in noise immission prognosis; Part II: Evaluation by Measurements. In *Proc. of Euronoise 2018* , pages 2077–2084, Crete, Greece, 2018.

[8] DIN ISO 38457:2025-05. *Acoustics - Software for the calculation for workspaces - Quality assurance of software-implemented methods*.

[9] H. A. Bethe. Theory of Diffraction by Small Holes. *The Physical Review*, 66(7-8):163–182, 1944.

[10] M. Biot and I. Tolstoy. Formulation of wave propagation in infinite media by normal coordinates with an application to diffraction. *J. Acoust. Soc. Am.*, 29:381–391, 1957.

[11] Z. Maekawa. Noise reduction by screens. *Appl. Ac.*, 1:157–173, 1968.

[12] DIN EN IEC 60268-16:2020. *Sound system equipment - Part 16: Objective rating of speech intelligibility by speech transmission index*.

[13] VDI 3760. *Berechnung und Messung der Schallausbreitung in Arbeitsräumen*. VDI-Handbuch, February 1996.